OPEN

The Effect of Gadolinium-Based Contrast Agents on Longitudinal Changes of Magnetic Resonance Imaging Signal Intensities and Relaxation Times in the Aging Rat Brain

Claudia Green, PhD, Gregor Jost, PhD,* Thomas Frenzel, PhD,* Janina Boyken, PhD,* Carsten Schwenke, PhD,† and Hubertus Pietsch, PhD**

Objectives: The aim of the study was to investigate the possible influence of changes in the brain caused by age on relaxometric and relaxation time–weighted magnetic resonance imaging (MRI) parameters in the deep cerebellar nuclei (DCN) and the globus pallidus (GP) of Gd-exposed and control rats over the course of 1 year.

Materials and Methods: Twenty-five Wistar-Han rats were equally subdivided into 5 groups and initially received 8 injections on 4 consecutive days per week of either 3.6 mL/kg body weight saline (group I–III) or 1.8 mmol Gd/kg body weight gadobutrol (group IV) or gadodiamide (group V). T1- and T2-weighted scans, as well as relaxation maps, were acquired at 1 week (all groups); 5, 12, 20, and 26 weeks (saline II, gadobutrol, gadodiamide); and at 35, 44, and 52 weeks (saline III, gadobutrol, gadodiamide) after the last administration. Saline I was euthanized after 1 week, saline II after 26 weeks, and the remaining groups after 52 weeks. Signal intensities (SIs) were evaluated for the DCN/pons (P) and the GP/piriform cortex (PC) ratios, and relaxation times for the DCN and the GP. Brain tissue was extracted, and the gadolinium, iron, and manganese contents were quantified with inductively coupled plasma mass spectrometry (ICP-MS) and laser ablation–ICP-MS imaging.

Results: T1-weighted SI ratios did not show any significant trend with age in any region. The between-group analysis at 52 weeks resulted in a significant difference for the DCN/P and GP/PC region ratio between gadodiamide and its comparators. T1 relaxation times dropped with increasing age in the GP with a 10% to 20% difference between first and last measurement for all groups, and in the DCN <10% with a significant decrease for the gadodiamide group only (DCN: $P = 0.0158$). Group-related differences were observed at the last measurement time point for T1 values between gadodiamide and saline III in the DCN ($P = 0.0153$) and gadodiamide and gadobutrol in the GP ($P = 0.0287$). Analysis of the SI ratios of the T2-weighted images revealed a significant increase for the DCN/P and a decrease for the GP/PC with increasing age for all groups and no differences at 52 weeks after the last injection between groups. T2 values of the GP showed a significant linear decrease over time for all groups (saline I–III: $P = 0.0101$; gadobutrol: $P = 0.0001$; gadodiamide: $P = 0.0142$) in the aging rat brain. Quantitative imaging of manganese and iron by laser ablation–ICP-MS showed a linear increase for the saline groups in the GP for both metals (Fe: $P < 0.0001$; Mn: $P = 0.0306$) and in the DCN for manganese only ($P = 0.0187$), but no differences between groups at 52 weeks.

Conclusions: Extensive MRI evaluation did not reveal an indication of SI or relaxation time changes associated with multiple exposure to the macrocyclic-chelated GBCA gadobutrol in the DCN and the GP. With increasing age, a T1 and T2 shortening in the GP and an increase in T2-weighted SI ratio in the DCN/P, as well as a decrease in the GP/PC, were observed for all groups. Such age-related changes can potentially bias MRI results as an indicator for gadolinium presence in the brain.

Key Words: magnetic resonance imaging, gadolinium, brain, contrast agent, aging

(*Invest Radiol* 2022;57: 453–462)

The use of gadolinium-based contrast agents (GBCAs) in contrast-enhanced magnetic resonance imaging (MRI) is well-established in clinical routine and of preeminent diagnostic and prognostic value in medical imaging. Within the last decade, numerous preclinical and clinical studies have addressed a chelate- and dosage-dependent causal relationship between GBCA administrations and signal hyperintensity on unenhanced T1-weighted MRI scans for the dentate nucleus, or the deep cerebellar nuclei (DCN) in rats, and the globus pallidus (GP).[1–17] The prolonged presence of GBCAs in various tissue types, even in healthy individuals with normal renal function, stoked increased concerns and uncertainties in clinical practice about the general safety profile of GBCAs. For GBCAs with a linear structure, studies unequivocally showed a significant and persistent increase in unenhanced T1-weighted signal intensity (SI) and T1 shortening after cumulative doses of contrast agent[6,7,18–23] and has led to their suspension for clinical use in the European Union.[24] Macrocyclic GBCAs are considered more stable due to their higher kinetic inertness as compared with linear agents.[7,18,19,21,25–29] Magnetic resonance imaging metrics only serve as a surrogate measure for tissue Gd concentration, and the interpretation of MRI data is further complicated by varying influencing factors between studies, such as an interindividual gadolinium elimination period.[19] Most preclinical and clinical studies focused solely on a semiquantitative analysis of hyperintensities on native T1-weighted images, inherently influenced by diverse factors due to their relative nature, such as the need for and choice of a reference region. Evaluations of quantitative relaxometry data after exclusively serial macrocyclic CA administrations remain sparse with inconclusive results between studies.[30–37] Further, retrospective studies often lack age-matched control groups with no prior exposure to GBCAs. The reported ambiguous outcomes for macrocyclic GBCAs regarding T1 shortening spur the need for further thorough research.

Few dedicated studies identified multiple sources of imaging data variability from image acquisition to reconstruction to address and support resolving the controversial outcomes for patients with a history of serial GBCAs.[38–41] Recently, age-related SI changes have been investigated as a potential confounding variable of Gd-dependent hyperintense brain regions.[30,42,43] Aging processes that are not associated with neuropathology are known to alter the concentration and distribution of paramagnetic elements, such as iron and manganese, and result in

Received for publication October 23, 2021; and accepted for publication, after revision, December 8, 2021.

From the *Department of MR and CT Contrast Media Research, Bayer AG; and †SCO:SSiS Statistical Consulting, Berlin, Germany.

Conflicts of interest and sources of funding: C.G., G.J., T.F., J.B., and H.P. are employees of Bayer AG. C.S. is a consultant to Bayer AG on an honorary basis.

Correspondence to: Claudia Green, PhD, Department of MR and CT Contrast Media Research, Bayer AG, Muellerstr 178, Berlin 13353, Germany. E-mail: clgreen@web.de.

Supplemental digital contents are available for this article. Direct URL citations appear in the printed text and are provided in the HTML and PDF versions of this article on the journal's Web site (www.investigativeradiology.com).

Copyright © 2022 The Author(s). Published by Wolters Kluwer Health, Inc. This is an open-access article distributed under the terms of the Creative Commons Attribution-Non Commercial-No Derivatives License 4.0 (CCBY-NC-ND), where it is permissible to download and share the work provided it is properly cited. The work cannot be changed in any way or used commercially without permission from the journal.

ISSN: 0020-9996/22/5707–0453
DOI: 10.1097/RLI.0000000000000857

TABLE 1. Image Acquisition Parameters in the Order of Acquisition

	T2w	T1w	T2 Map	T1 Map
Sequence	2D TSE	3D TSE	SE	TSE-variable TI
TR/TI; TE, ms	5000; 95	500; 16	3000; 8.5–272	25, 1600, 300, 50, 1100, 100, 2400, 150, 700, 200, 4000, 500; 8.4
Slices	18	24	2	2
Flip angle, degrees	90	150	180	180
Resolution, mm	0.2 × 0.2 × 1.0	0.2 × 0.2 × 1.0	0.2 × 0.2 × 2.0	0.2 × 0.2 × 2.0

The entire image protocol took approximately 45 minutes per animal and session.

T2w, T2-weighted; T1w, T1-weighted; TSE, turbo spin echo; SE, spin echo; TR, repetition time; TI, inversion time; TE, echo time.

quantitative neurological changes of tissue-specific morphology and white matter hyperintensities.[44–46] These changes have been observed to affect various MRI metrics, such as T2 shortening in the gray matter nuclei and the basal ganglia as a result of increasing mineralization.[47–53]

Our preclinical long-term study aims to aid a comprehensive understanding of the controversial discussion of quantitative and semiquantitative MRI SI changes after cumulative GBCA exposure through multiple, multiparametric MRI of rat brains. For this purpose, we repetitively assessed unenhanced T1/T2 maps and T1/T2-weighted MRI scans over the course of 1 year in healthy rats that had received repeated injections of either a macrocyclic GBCA, a linear GBCA, or saline. To validate our results, we included ex vivo tissue analysis of gadolinium, iron, and manganese concentrations by laser ablation inductively coupled plasma mass spectrometry (LA-ICP-MS). We further aimed to discriminate between natural age-dependent MRI parameter changes and those externally driven due to serial administration of contrast agents.

MATERIALS AND METHODS

Animals

All animal experiments were conducted according to the guidelines of the German Animal Welfare Act and with the approval of the local state animal welfare committee. Animals were socially housed under a fixed 12:12-hour light/darkness cycle under standard laboratory conditions with ad libitum access to standard food and water. In total, 25 Han-Wistar rats (Crl:WI; male; ~8–9 weeks), weighing 211 to 248 g at the start of the experiment, were obtained from Charles River (Sulzfeld, Germany). Imaging procedures were performed under continuous anesthesia with 1.5% isoflurane (Baxter GmbH, Unterschleissheim, Germany) in a mixture of 50/50 N_2O/O_2. For exsanguination, additional analgesic treatment was given through a mixture of 1:18 xylazine hydrochloride (20 mg/mL, Rompun; Bayer Vital GmbH, Leverkusen, Germany) and ketamine hydrochloride (100 mg/mL, Ketavet; Pfizer, Pharmacia GmbH, Berlin, Germany) of 1.1 mL/kg body weight.

Study Design

The 25 rats were randomly divided into 5 equally sized groups before the start of the experiment. Each group received 8 intravenous injections for 4 consecutive days per week over a period of 2 weeks of the following treatment: groups saline I–III received 3.6 mL/kg body weight saline, the gadobutrol group (Gadovist; Bayer Vital, Leverkusen, Germany), and the gadodiamide group (Omniscan; GE Healthcare Buchler & Co, Braunschweig, Germany) 1.8 mmol Gd/kg body weight (equivalent to 1.8 mL/kg and 3.6 mL/kg body weight and corresponding to a triple clinical standard dose after body surface adaption), respectively.

Repeated MRI of the brain was performed at 1, 5, 12, 20, 26, 35, 44, and 52 weeks post last injection (PI). All MRI experiments were conducted on a clinical 1.5 T MRI system (Magnetom Avanto Fit; Siemens Healthcare GmbH, Erlangen, Germany) using a dedicated 2-channel quadrature volume resonator with an inner diameter of 72 mm (Rapid Biomedical GmbH, Rimpar, Germany). After initial anatomical reference images, a serial acquisition of a T2-weighted and T1-weighted image, as well as scans for the calculation of a T2- and a T1-map, was acquired with the parameters shown in Table 1.

Two additional saline groups were included in the MRI. These were euthanized before the end of the study—after 1 week (group I) and 26 weeks (group II)—to quantify metals in the brain during aging. All remaining groups were euthanized after the last imaging at 52 weeks PI. An

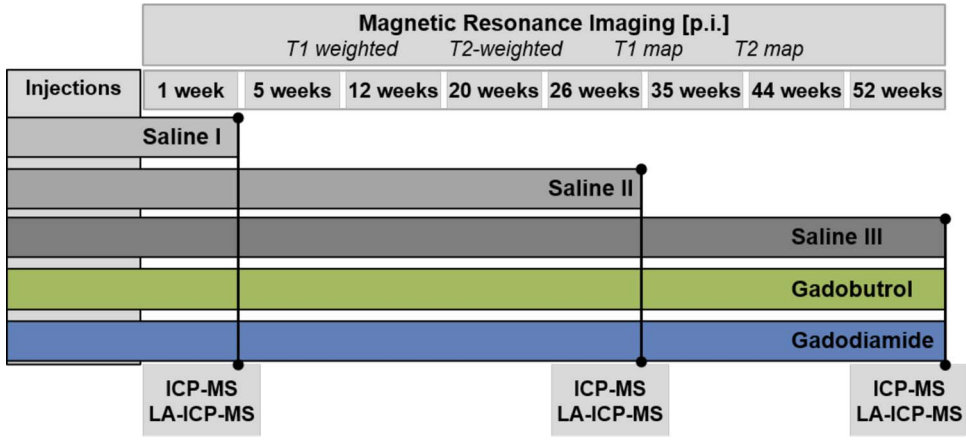

FIGURE 1. Study design: 25 rats were subdivided into 5 groups receiving 8 injections over the time course of 2 weeks of either saline (saline I, saline II, saline III), gadobutrol, or gadodiamide, respectively. Magnetic resonance imaging (MRI) was performed at 1, 5, 12, 20, 26, 35, 44, and 52 weeks after the last injection. At the end of the indicated study periods, animals were killed and inductively coupled plasma mass spectrometry (ICP-MS), as well as laser ablation inductively coupled plasma mass spectrometry (LA-ICP-MS) analysis was conducted to quantitatively assess metal content in the brain.

© 2022 The Author(s). Published by Wolters Kluwer Health, Inc.

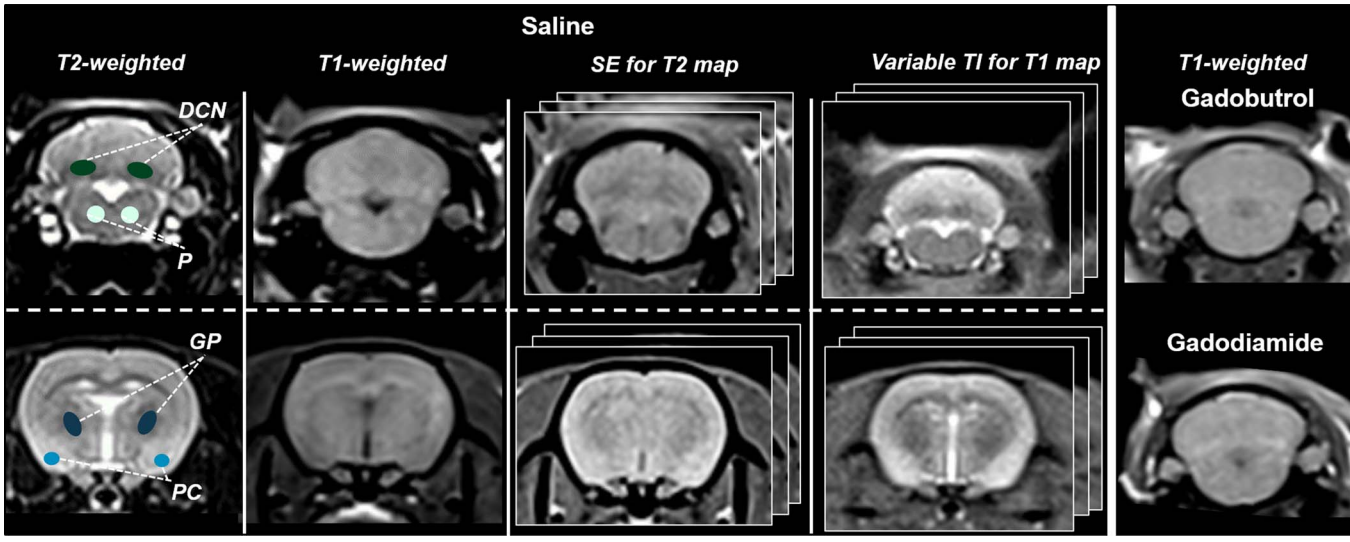

FIGURE 2. Columns 1–4: Representative MRI scans of a rat in saline I at 1 week after the last saline injection with exemplary region of interest (ROI) delineation (echo time of 8.5 milliseconds shown for spin echo for T2 map; inversion time of 200 milliseconds shown variable inversion time for T1 map). Column 5: Representative T1-weighted images of a gadobutrol and a gadodiamide animal of the deep cerebellar nuclei (DCN) region.

overview of the study design is provided in Figure 1, and sample MRI scans are shown in Figure 2. The animals were euthanized by exsanguination, and the brain tissue was taken. The hemispheres were separated for the measurement of total gadolinium (Gd), manganese (Mn), iron (Fe), and Zinc (Zn) concentrations by ICP-MS and for determination of spatially resolved Gd, Mn, and Fe content distribution by LA-ICP-MS.

Image Evaluation

T1 and T2 maps were calculated with an in-house software ELMAR Viewer v.1.6 (Fraunhofer Mevis, Berlin, Germany) and on the Siemens workstation. Signal intensities and relaxation times were obtained from manually drawn regions of interest (ROIs) around the DCN and the GP on both hemispheres on a workstation (syngo.via Siemens Healthcare GmbH). On the T1/T2-weighted images, reference SIs from ROIs around the pons (P) and the piriform cortex (PC) were obtained additionally, and the DCN-P/GP-PC ratio was calculated as the average from both hemispheres, respectively, to account for intraindividual noise fluctuations. Both reference regions were chosen because they showed the lowest gadolinium concentration after visual inspection of the LA-ICP-MS images. The obtained values were finally group-averaged per time point, with no further distinction being made between the saline groups.

ICP-MS Measurements for Metal Concentrations

Total concentrations of gadolinium, iron, manganese, and zinc were determined in the cerebrum, cerebellum, brain stem, and the olfactory bulb (OB) as described previously.[19] The brain sections were manually homogenized and weighed, and aliquots of 10 mg were then mixed with 50 µL of 100 nM $Tb(NO_3)_3$ as an internal standard. After the samples were dried for 2 hours at 95°C, 50 µL of concentrated nitric acid (65% HNO_3, Fisher Chemical, Thermo Fisher Scientific, Schwerte, Germany) and 30 µL of hydrogen peroxide (30% H_2O_2, VWR Chemicals) were added, and mixtures were heated in a microwave oven (Mars 5 Xpress; CEM, Kamp-Lintfort, Germany). Once the samples cooled down to room temperature, 920 µL of 1% HNO_3 and 0.01% Triton X 100 was added. The final diluted and centrifuged samples were measured by ICP-MS (Agilent 8900; Waldbronn, Germany) using the reaction cell with 5.5 mL/min He to suppress interfering ions. The method has a lower limit of quantification of 0.01 nmol Gd/g and 0.1 nmol Mn/Fe/Zn per gram tissue. In a last step, average and median values per group and neuroanatomical region were determined.

LA-ICP-MS for Spatially Resolved Metal Distribution

Spatially resolved Gd, Fe, and Mn concentrations were determined with LA-ICP-MS for specific quantitative analysis of metal content within the DCN and GP region. One hemisphere was embedded in Tissue Tek O. C.T. Compound (Sakura Finetek; Alphen aan den Rijn, the Netherlands) directly after extraction and snap frozen with isopentane. The tissue was cryosectioned in 10 µm thin coronal slices and mounted on Superfrost Ultra Plus adhesive glass slides (Menzel Glaeser, Braunschweig, Germany). Laser ablation was performed with an inductively coupled plasma mass spectrometer (Thermo iCap RQ ICP-MS, Thermo Fisher Scientific, Waltham, MA) coupled to a laser ablation system (ESI NWR 213; New Wave Research, Fremont, CA), as previously described.[19,54] Images were generated, and the elements were identified with ImaJar software (kindly provided by Robin Schmid and Uwe Karst, University of Muenster, Germany). Gelatin standards containing known Mn/Fe/Gd concentrations were sliced in the same way as the tissue and measured in each session for calibration and quantification in tissue samples. Regions of interest were localized and drawn on the Fe/Mn images around the DCN and the GP for local quantification and statistics.

Statistical Evaluation

Data of a total of 25 rats with 5 rats per group were used for the analyses. All data are shown as mean ± standard deviation unless stated otherwise. Statistical results are reported as least square (actual) mean differences with 95% confidence intervals (CIs) from analysis of variance or mixed models with repeated measures as appropriate. For the T1-weighted and T2-weighted images, the SI ratios DCN/P and GP/PC were assessed for changes over time up to week 52 using mixed models with repeated measures and for differences at week 52 between saline III, gadobutrol, and gadodiamide using analysis of variance. The T1-map and T2-map of the DCN and GP were analyzed in the same manner. Normality was assessed by visual inspection taking into account that for analyses in week 52, a total of only 15 rats were included, meaning results had to be interpreted with care. Analyses were conducted using SAS 9.4 (SAS Institute Inc, Cary, NC) and GraphPad Prism 8.0.2 (GraphPad Software, San Diego, CA).

RESULTS

Twenty-four of 25 rats successfully completed the study protocol. One rat from the saline III group was excluded from the study after

© 2022 The Author(s). Published by Wolters Kluwer Health, Inc.

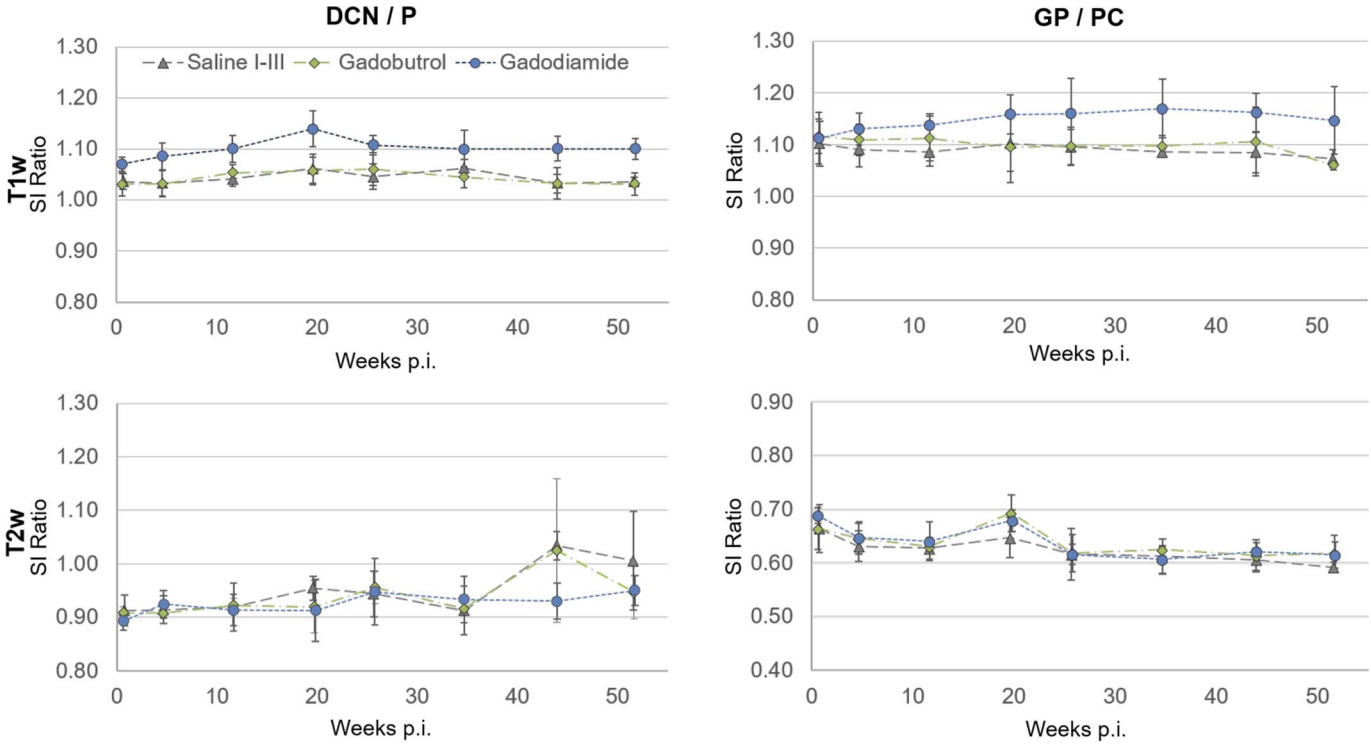

FIGURE 3. Deep cerebellar nuclei/pons (P) and globus pallidus (GP)/piriform cortex (PC) signal intensity ratios analyzed on T1-weighted (upper row) and T2-weighted (bottom row) images for all groups, presented over the study time course in weeks with standard deviations. Values of saline groups I–III are summarized (mean values 1 week: n = 15, 2–26 weeks: n = 10, 27–52 weeks: n = 5).

the MRI measurement in week 44 PI due to a treatment-unrelated neoplasia in the right mandibular gland. Two rats of the gadodiamide group showed mild to moderate hair loss at 4 weeks after the last injection, with a recovery period of up to 4 months and no further adverse effects. Animals weighed on average 222.6 ± 8.4 g at the start of the experiment and 544.9 ± 68.7 before the last MRI measurement in week 52 PI (saline III, gadobutrol, and gadodiamide) with no statistically significant difference between the groups.

QUANTITATIVE MRI ANALYSIS

T1- and T2-Weighted Images

The T1- and T2-weighted temporal SI changes of the DCN/P and GP/PC ratios are presented in Figure 3. Signal intensity ratios of the T1-weighted images started in the DCN/P at 1.05 ± 0.03 for saline I–III, 1.06 ± 0.03 for gadobutrol, and 1.08 ± 0.02 for gadodiamide, and in the GP/PC at 1.10 ± 0.04 for saline I–III, 1.12 ± 0.03 for gadobutrol, and 1.11 ± 0.05 for gadodiamide. Both T1-weighted ROIs were stable, with no significant effect noted with increasing age and less than 4% changes between the first and the last measurement time point for all groups (Table 2). Investigating GBCA-associated differences, the between-group analysis for the T1-weighted images of the last measurement time point revealed a distinctly higher SI for the gadodiamide group of the DCN/P (1.10 ± 0.02) and the GP/PC (1.15 ± 0.07) ratio compared with the saline III group (DCN/P = 1.04 ± 0.01, P = 0.0003; GP/PC = 1.07 ± 0.02, P = 0.0211) and the gadobutrol group (DCN/P = 1.03 ± 0.02, P = 0.0001; GP/PC = 1.06 ± 0.01, P = 0.0067). This difference is already evident from the second measurement time point at 5 weeks after the last injection onwards. The

TABLE 2. Overview of the Mixed Models Regression Analysis With Repeated Measures for the DCN/P and GP/PC Ratios of the T1-Weighted and T2-Weighted Images, and the DCN and GP T1 and T2 Relaxation Times

		DCN/P		GP/PC			DCN		GP	
		Slope	P	Slope	P		Slope	P	Slope	P
Saline	T1w	0.00003	0.2837	−0.0001	0.2313	T1 map	0.0233	0.5851	−0.3285	*<0.0001*
Gadobutrol		−0.00001	0.7258	−0.0001	0.0684		−0.0700	0.2340	−0.2263	*<0.0001*
Gadodiamide		0.00005	0.2038	0.0001	0.0938		−0.1221	*0.0158*	−0.2676	*<0.0001*
Saline	T2w	0.0003	*<0.0001*	−0.0002	*0.0001*	T2 map	0.0026	0.3782	−0.0047	*0.0101*
Gadobutrol		0.00021	*0.0125*	−0.0001	*0.0034*		−0.0012	0.8395	−0.0108	*0.0001*
Gadodiamide		0.00011	*0.0317*	−0.0002	*0.0004*		−0.0006	0.8771	−0.0146	*0.0142*

P values <0.05 are considered significant and displayed italicized. The slope of the regression analysis function provides shows the steepness and direction.
DCN, deep cerebellar nuclei; P, pons; GP, globus pallidus; PC, piriform cortex; T1w, T1-weighted; T2w, T2-weighted.

© 2022 The Author(s). Published by Wolters Kluwer Health, Inc.

DCN/P and GP/PC SI ratios (SIRs) of the gadobutrol group are very similar to that of the saline III group, with no relevant/significant differences. The T2-weighted SIs showed a significant increase for the DCN/P ratios and a decrease for the GP/PC ratio for all groups with increasing age as shown in Table 2. No relevant differences between groups were found for the T2-weighted SIRs ($P > 0.15$).

T1 and T2 Mapping

T1 relaxation times for the GP (Fig. 4, top row) were 794.7 ± 28.3 milliseconds (saline I–III), 756.1 ± 21.5 milliseconds (gadobutrol), 767.9 ± 8.5 milliseconds (gadodiamide) at the first MRI. T1 values dropped significantly over time in all 3 groups with an averaged difference between first and last measurement value of −19% for the saline and gadodiamide groups and −11% for the gadobutrol group. T1 values for the cerebellar nuclei remained stable in the first 6 months of the study and presented larger fluctuations in relaxation times for the second half of the measurement time points, with a significant decrease for gadodiamide only ($P = 0.016$, see Table 2). Between the last and first MRI session, the mean decrease in DCN T1 relaxation times were 2%, 9%, and 8% for saline I–III, gadobutrol, and gadodiamide, respectively. Contrast agent–associated changes were observed for gadodiamide group only. Significant T1 shortening was observed at 52 weeks PI for the gadodiamide animals compared with the saline group III in the DCN (difference, 67.7 milliseconds; CI, 15.71–119.69; $P = 0.015$) and to the gadobutrol animals in the GP (difference, 32.87 milliseconds; CI, 4.11–61.62; $P = 0.029$).

T2 relaxation times of the cerebellar nuclei were 83.1 ± 2.4 milliseconds (saline I–III), 84.2 ± 5.1 milliseconds (gadobutrol), and 82.0 ± 2.7 milliseconds (gadodiamide) at the first MRI and fluctuated over the course of the study with no linear trend and less than 2% changes in mean value between the first and last measurement (Fig. 4, bottom row). No differences between the study groups were noted at the end of the study. T2 relaxation times for the GP were 81.5 ± 1.3 milliseconds (saline I–III), 83.2 ± 2.0 milliseconds (gadobutrol), and 80.8 ± 0.7 milliseconds (gadodiamide) at the first MRI. These values decreased slightly over time (≤4%). The resulting negative slope was significantly different from zero for all groups (Table 2). At the end of the study, T2 relaxation times for the GP in the gadodiamide animals showed an actual mean difference to saline III of 2.87 milliseconds ($P = 0.02$) and a 2.59 milliseconds difference to gadobutrol ($P = 0.03$).

Quantification of Metal Content by ICP-MS and LA-ICP-MS

Total Metal Content in the Brain

Total concentrations of Gd, Fe, Mn, and Zn in the cerebellum, cerebrum, brain stem, and OB were analyzed using ICP-MS. Gadolinium concentrations in animals without exposure to GBCA (saline I–III) were below the limit of quantification (0.01 nmol Gd/g tissue) in all brain sections, except for 1 animal from saline II, which was slightly above the LOQ. Exemplary LA-ICP-MS images of Gd distribution in the gadobutrol and gadodiamide groups, as well as Gd concentrations of group III–IV are shown in Supplemental Figure 1 (http://links.lww.com/RLI/A680). The average values of the gadobutrol animals at 52 weeks PI ranged from 0.07 ± 0.01 nmol/g in the brain stem to a maximum of 0.25 ± 0.03 nmol/g in the OB. Gadodiamide animal gadolinium concentrations were 1 order of magnitude higher with 1.00 ± 0.3 nmol/g in the brain stem, 3.11 ± 0.89 nmol/g in the cerebrum, 3.74 ± 0.52 nmol/g in the cerebellum, and 15.11 ± 1.51 nmol/g in the OB. At the last measurement time point, no group differences were observed between the concentrations for the endogenous metals Fe, Mn, and Zn. For Fe, a linear regression analysis revealed a significant increase in metal concentration with increasing age in the saline groups

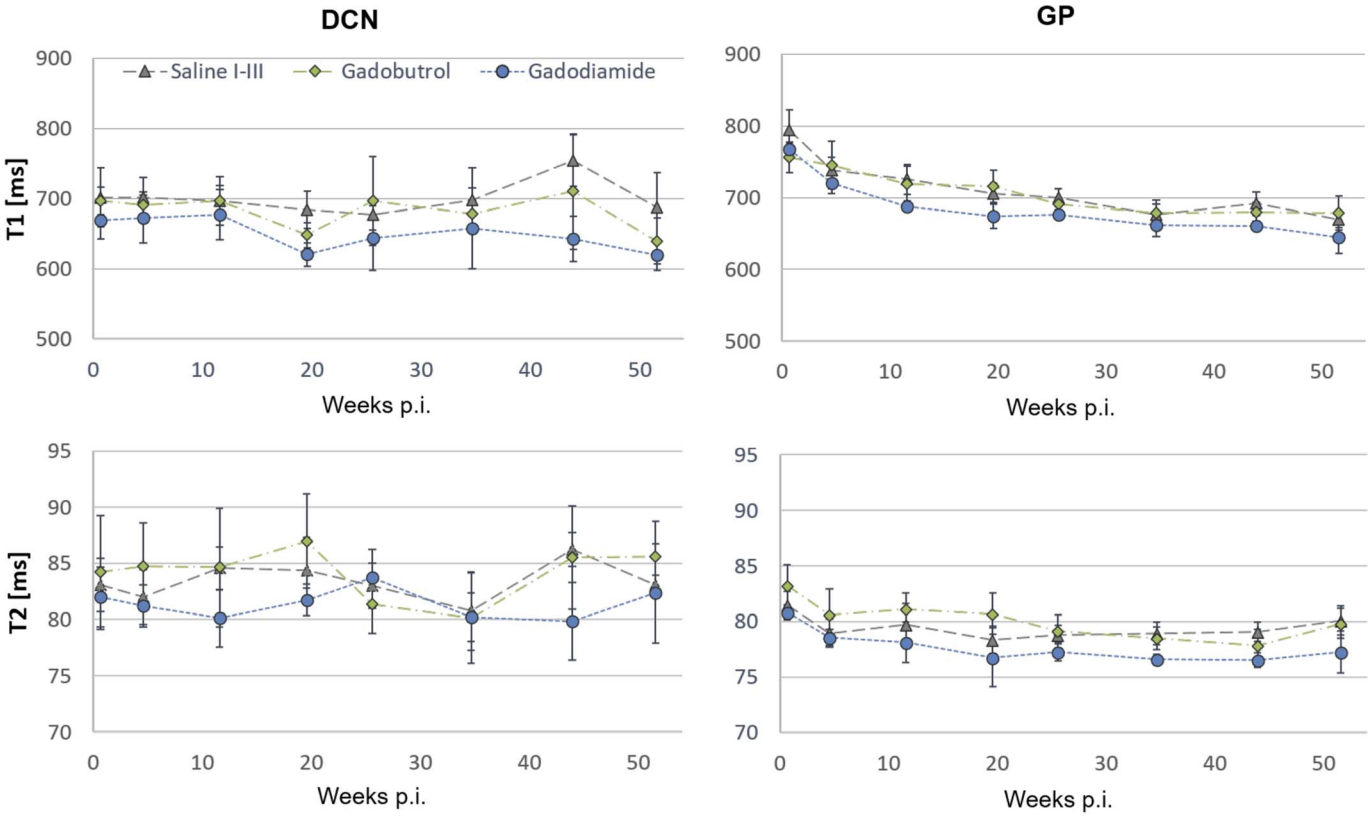

FIGURE 4. Relaxometric data (mean ± standard deviations) for ROIs in the DCN on the left side and the GP on the right side presented over time with standard deviations. The results from all saline groups were averaged per time point.

© 2022 The Author(s). Published by Wolters Kluwer Health, Inc.

in all measured brain regions but the brain stem (cerebellum: slope = 2.89 nmol/g per week, $P \leq 0.0001$; cerebrum: slope = 1.33 nmol/g per week, $P = 0.0025$; OB: slope = 4.09 nmol/g per week, $P \leq 0.0001$). Fe concentrations predominantly increased between the first week and the 6-month measurement time point in the cerebellum, cerebrum, and OB by 27.9% ± 2.5% on average and resulted in an overall increase from earliest to latest time point of 40.3% ± 13.0%, whereas brain stem concentrations remained at a rather similar level, with a maximal increase of 12.9%. Zn concentrations showed an age-dependent decreasing trend with a significant effect in the cerebellum and the brain stem (cerebellum: slope = −0.27 nmol/g per week, $P = 0.0263$; brain stem: slope = −0.52 nmol/g per week, $P = 0.0187$), most pronounced between saline I and saline II with only small changes thereafter. No significant change in manganese concentrations was detected for the saline groups over time, although values of the cerebellum, the cerebrum, and the OB showed an increase of 12.5% ± 5.8%/14.5% ± 7.9% between saline I and saline II/saline III. Median values of all groups and regions with interquartile ranges are summarized in Table 3.

Laser Ablation Inductively Coupled Plasma Mass Spectrometry

Spatially resolved distribution of gadolinium, iron, and manganese were assessed with LA-ICP-MS on half-hemisphere brain tissue slices. Exemplary images of both regions from each group, as well as group-averaged local quantifications of Fe and Mn concentrations in both regions, are summarized in Figure 5. Cerebrum tissue samples from 4 animals in saline II and 1 animal in saline III could not be processed due to incorrect embedding. Consistent with the quantitative ICP-MS results, statistical analysis showed no contrast agent-associated differences of endogenous elements between groups at 52 weeks PI for Mn and Fe. A significant age-dependent linear increase in concentration was noted for the saline groups over the course of the study in the GP for Fe and marginally for manganese (Fe: slope = 8.771 nmol/g per week, $P < 0.0001$; Mn: slope = 0.03487 nmol/g per week, $P = 0.0306$) and in the DCN for Fe only (slope = 9.346 nmol/g per week, $P = 0.0011$). No residual gadolinium was detected for the saline III and gadobutrol group in the GP, but a minimal concentration above the detection limit of 0.3 ± 0.4 nmol/g tissue in the DCN for gadobutrol (Supplemental Fig. 1, http://links.lww.com/RLI/A680, upper row). The average gadolinium concentration in the animals that received gadodiamide at 1 year after the last injection was considerably higher, with 11.8 ± 2.4 nmol/g tissue in the GP and 18.7 ± 7 nmol/g tissue in the DCN.

DISCUSSION

Clinical and preclinical studies have been conducted to evaluate the short- and long-term effect of repeated GBCA injections on MRI parameters, to assess a potential safety concern regarding gadolinium accumulation in the brain.[1–23,25,27–38,54–56] The conclusiveness of these studies is challenged by controversial results regarding the existence of permanent changes of T1-weighted SIs and T1 values after exclusively serial macrocyclic CA administrations,[30–37] as well as the correlation of age with a signal change in T1-weighted MRI,[30–33,42,43] specifically in the GP and DCN region of the brain.

In the present rat brain study, we targeted a conclusion of these controversies, by exploring changes in multiple MRI parameters during a 1-year, treatment-free period after initial repetitive administration of either saline, gadobutrol, or gadodiamide. We set a specific focus on the saline control groups to evaluate naturally occurring parameter variations with age in the DCN and the GP that might have to be considered a confounding variable in the common analysis of Gd-dependent MRI findings.

Our study design only included posttreatment time points with saline groups as the major comparator. Summarizing in that regard, ex vivo metal quantification revealed a strong increase in Fe concentration over the course of time in the Gd-naive animals, with no differences between the groups at the last measurement time point. Further, we found no increase in the SI ratios with age in the DCN/P and the GP/PC regions on the T1-weighted images within each study group starting from 1 week to 52 weeks after the last treatment, but a consistent decrease on the T2-weighted images, along with a significant linear decrease in T1 and T2 relaxation times in the GP for all groups. No significant difference between the saline group and the macrocyclic GBCA group was detected for any parameter. Consistently higher/lower values were observed between the gadodiamide group and its comparators for the T1-weighted scan and the relaxation maps, respectively.

In line with our findings, 2 studies did not find any differences in T1 relaxation times between a Gd-naive control group and patients with a history of gadobutrol injections, even after frequent administrations and an interval time between the last GBCA dose and the investigated native T1 MRI scan of only 119 days on average.[30,33] Further in these studies, in a multivariate regression analysis accounting for different confounding variables, no association between the number of gadobutrol injections and T1 relaxation time was found.[30,33] Conversely, clinical studies by Saake et al[32] and Kang et al[31] reported a T1 shortening in the GP but not the DCN, positively correlated with gadobutrol doses, albeit in the absence of visual signal alterations. However, both studies

TABLE 3. Total Median Concentrations of Iron, Manganese, and Zinc Measured in the Cerebellum, the Cerebrum, the Brain Stem, and the Olfactory Bulb With Inductively Coupled Mass Spectrometry for All Groups Separately

Element	Neuroanatomical Region	Saline I (1 wk PI)	Saline II (26 wk PI)	Saline III (52 wk PI)	Gadobutrol (52 wk PI)	Gadodiamide (52 wk PI)
Zn	Cerebellum	318 (304–341)	411 (410–421)	(26 weeks PI)	479 (473–479)	462 (459–521)
	Cerebrum	265 (255–270)	356 (323–358)	343 (329–344)	328 (327–364)	344 (333–361)
	Brain stem	286 (246–291)	313 (287–316)	318 (295–327)	307 (278–324)	307 (279–315)
	Olfactory bulb	442 (394–449)	500 (500–539)	617 (616–626)	612 (576–623)	629 (626–631)
Mn	Cerebellum	8.4 (8.1–8.4)	9.1 (8.1–10.4)	9.0 (8.8–9.1)	9.4 (9.4–9.5)	8.7 (8.7–9.37)
	Cerebrum	7.1 (7.1–7.7)	9.1 (8.5–9.1)	8.3 (8.2–8.6)	8.6 (8.3–8.6)	8.3 (7.8–8.4)
	Brain stem	9.4 (8.7–10.3)	8.7 (8.0–9.2)	8.9 (8.7–8.9)	9.3 (8.8–9.4)	8.6 (8.3–9.4)
	Olfactory bulb	8.2 (7.9–8.6)	8.7 (8.1–9.4)	9.4 (9.3–9.5)	10.1 (9.5–10.1)	8.6 (8.4–8.9)
Fe	Cerebellum	158 (156–159)	140 (13–142)	139 (138–149)	144 (141–144)	148 (148–149)
	Cerebrum	184 (180–195)	190 (169–194)	170 (169–176)	172 (169–173)	175 (174–179)
	Brain stem	115 (112–143)	102 (95–106)	97 (94–99)	95 (95–96)	95 (93–96)
	Olfactory bulb	193 (169–197)	166 (162–174)	179 (175–193)	166 (161–188)	170 (155–170)

Interquartile ranges are shown in round brackets.

© 2022 The Author(s). Published by Wolters Kluwer Health, Inc.

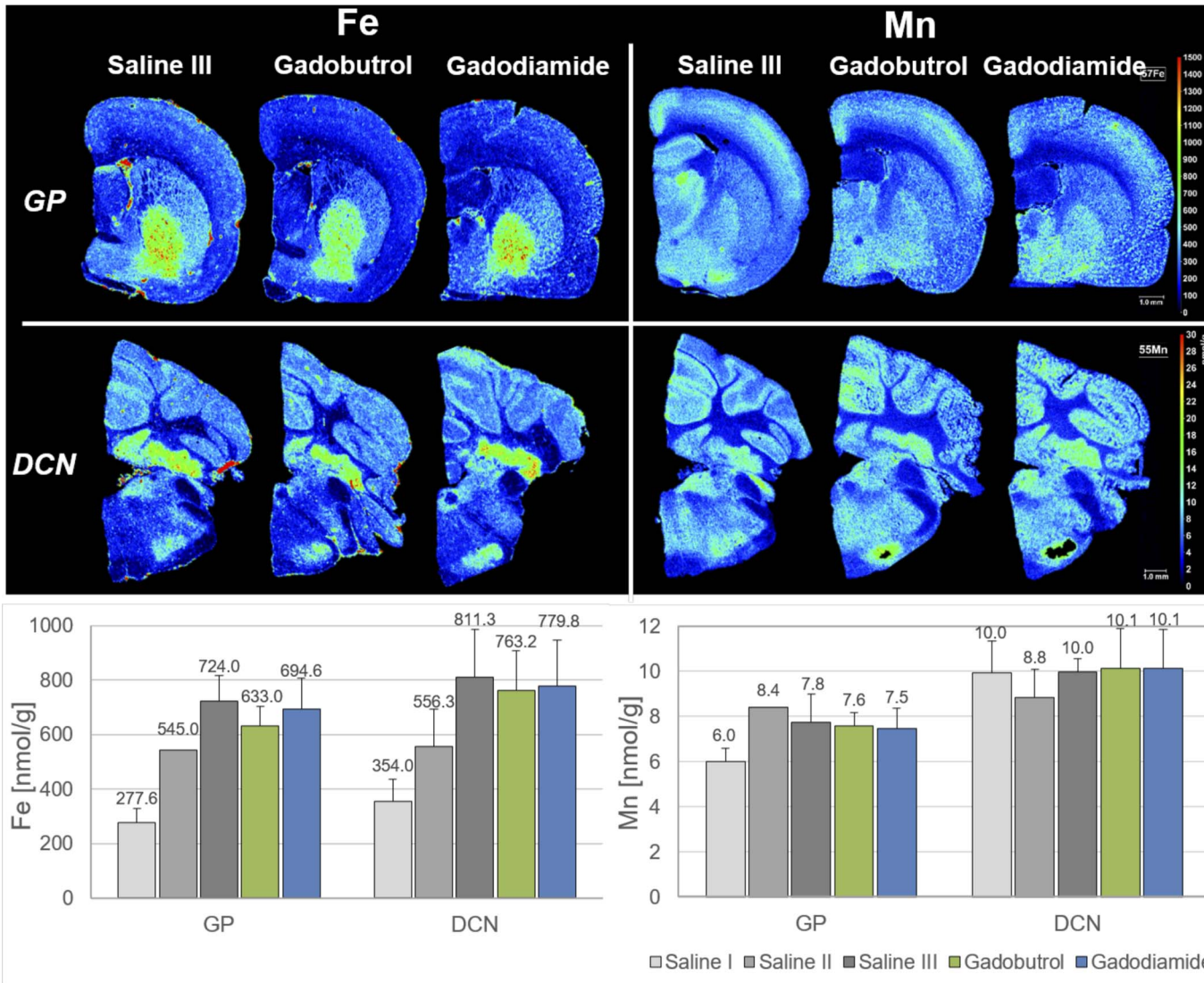

FIGURE 5. Results from the LA-ICP-MS analysis of iron (left side) and manganese (right side) within the GP and the DCN. Top, Representative images of metal concentrations for the saline III, gadobutrol, and gadodiamide animals at 52 weeks post last injection. Bottom, Quantitative analysis results for all groups (saline I: 1 week PI; saline III: 26 weeks PI, saline III: 52 weeks PI), presented as bar charts with mean ± standard deviation.

also report possible confounding points in question. Saake et al[32] also presented the opposite finding, that is, T1 prolongation compared with the respective control group for a study group with renal impairment, with no clear interpretation. In addition, Kang et al[31] did not include a reference group without gadolinium exposure and, due to limited available data, also included patients with a previous history of GBCAs other than gadobutrol. Interestingly, a T1 decline was also found in the GP in our study, but not in the DCN. However, this is not related to the GBCA treatment, as it was also observed in the saline groups, demonstrating the importance of an age-matched control group.

The absence of significant differences between the gadobutrol group and the control group on the T1-weighted images, as shown in our results, has previously been reported in most clinical[1,30–33,36,37,43] and preclinical rat studies,[16,19] where no correlation between the number of gadobutrol administrations and SIRs could be identified. Only a few retrospective clinical studies reported an increased SIR after multiple gadobutrol doses on unenhanced T1-weighted images in the dentate nucleus[9,17,57,58] and the GP,[9] not confirmed in our findings.

A retrospective GBCA study in patients by Quattrocchi et al[42] specifically investigated the effect of age on the T1-weighted SIRs in the brain. They found a negative correlation for the CN/pons ratio, along with a positive correlation for the GP/thalamus SIR in the Gd-naive control groups and the patient cohort that received gadodiamide, with the latter presenting steeper slopes. We did not find a significant age-related change in the T1-weighted SIRs in any of the investigated groups and thus cannot confirm their result in rodents. Further, the observed GP T1 shortening of the saline group with increasing age in our study differs from the literature data of studies in patients. In line with our results, one study describes a negative impact of age on the T1 ratio of the dentate nucleus-to-pons and GP-to-frontal white matter lobe, and a second study on the T1 in the GP.[33,43] However, age has also been reported to be significantly associated with an increase in T1 relaxation time in 3 clinical studies for the GP,[30–32] the DN, and the thalamus.[30,31]

Increasing or decreasing MRI metrics within a group over time, specifically if observed in the control group, may be associated with normal physiological aging processes in the brain. Clinically observed

© 2022 The Author(s). Published by Wolters Kluwer Health, Inc.

age-dependent MRI parameter variations have been related to increasing mineral deposition in brain tissue, progressive demyelination, and gray matter volume shrinkage,[49,59–63] however, with a high interindividual variability. The significant increase in Fe concentration detected here in the saline groups in both ROIs with increasing age, as measured by LA-ICP-MS, reflects and aligns very well with the observed T1 and T2 shortening in the GP, along with the hypointensity in GP/PC SIR on the T2-weighted images.[52,64] This increase could be an age-related factor explaining discrepancies between the aforementioned publications.

No T2 differences were found in our study for the macrocyclic group compared with our control group, and no association with Gd presence was concluded accordingly. This finding is along with prospective clinical literature data of patients after exclusive repetitive injections of gadobutrol or gadoterate meglumine (Dotarem; Guerbet, Aulnay-sous-Bois, France) including the GP and the DCN in their analysis.[32,55]

Only very limited articles are available in the literature on T2-weighted SIRs and relaxometric values after serial GBCA exposure and with regards to aging processes in the ROIs investigated here. Müller et al[33] did not find any correlation with age in the T2 ratio of the dentate nucleus to the pons, or the GP to the frontal normal white matter in gliobastoma patients, whereas clinical data from Krug et al[43] identified significant T2 shortening in the caudate nucleus, nucleus ruber, and the substantia nigra.

On average, animals that received the linear nonionic GBCA gadodiamide showed consistently higher SIRs and lower T1 values relative to animals in the saline and gadobutrol groups for both analyzed regions. The hyperintensity on unenhanced T1-weighted images after repeated administration of linear GBCAs has been previously investigated in multiple studies and confirmed by elemental tissue Gd analysis, specifically in tissue susceptible to mineral deposits, such as the dentate nucleus and the basal ganglia.[3,7,12–14,16,19,22,23,30,42,49,54] A few studies further investigated T1 relaxometry changes and confirmed the significant T1 shortening observed in the gadodiamide group compared with the control group.[22,34,55,56] Our imaging results are also confirmed by ex vivo LA-ICP-MS analysis of elemental gadolinium concentration, where we found no residuals in the GP and only trace concentrations in the DCN of the gadobutrol animals, but considerably higher concentrations in both regions in the gadodiamide animals.

Our study has several inherent limitations. The evaluation of human studies is often narrowed to the analysis of SIRs on T1-weighted images, and the high variability between patient medical histories regarding measurement techniques, GBCA injections, pathologies, and therapeutic interventions introduces many variables to consider and may have a significant impact on the results. Compared with human studies in clinical settings, animal studies have the advantage of a regulated and controlled environment with reduced confounding variables. However, despite these advantages, translatability is limited. In our study, we only used healthy rats and are not able to reflect any underlying pathological conditions, nor can we exactly match a certain age range equivalent to humans. Second, animal studies are ethically conducted with the fewest animals necessary for a specific research question. Our statistical analysis is thus based on a minimum number of animals. To obtain a more reliable outcome in the statistical models used, more observations would be needed. The validity of the statistical results should therefore be interpreted with care. We also used a repetitive GBCA dosing regimen of the maximum recommended dose for humans after body surface normalization according to Food and Drug Administration recommendations, as previously described.[19,65] The translated human cumulative dose given equates to 2.4 mmol/kg body weight within a very short time interval of only 2 weeks. Furthermore, limited by an acceptable scan time and the inclusion of single-slice acquisition sequences in our scan protocol, we could not confidently cover the thalamus, commonly used as an intensity reference region for the GP. Instead, we chose the piriform cortex based on our visual inspection of the ex vivo metal quantification, where we did not find deposits of gadolinium or Fe with increasing age. We thus do not expect a distinct outcome compared with the thalamus region. Nonetheless, we cannot exclude a certain variability. In this study, we evaluated parameter changes over time in comparison to a control group and do not consider pretreatment and posttreatment effects associated with GBCA exposure. We set one focus on the saline-treated control group and limited the animal number by not considering GBCA-treated groups with a survival time of 1 week PI and 26 weeks PI. As a result, we do not provide ex vivo results of metal concentrations and distribution of these groups and cannot compare changes in Fe concentrations of GBCA-treated animals between time points. Another limitation is based on the image acquisition itself, as we chose our sequences based on best performance under a certain total scan time restriction. As a result, we do not directly replicate clinical conditions, even for the simple reason that the coil used is specifically designed for small animals. It has been shown that the choice of sequence, the coil used, and postacquisition intensity corrections may have an impact on the assessment of MRI metrics.[39]

In conclusion, we observed an age-related decrease of T1 and T2 values in the GP in rats. In addition, we present an increase in T2-weighted SIR in the DCN/P and a decrease in the GP/PC over time. Therefore, age must be considered as a confounding factor when evaluating MRI SIRs or relaxometric data as surrogate for the presence of Gd in the brain. Further, our long-term MRI analysis showed no gadolinium presence in the dentate nucleus and the GP after serial application of the macrocyclic-chelated GBCA gadobutrol. In line with our MRI results, ex vivo metal quantification showed a significant increase in Fe concentration in Gd-naive animals within a 1-year observation period and did not present significant differences between groups at the end of the study.

ACKNOWLEDGMENT

The authors gratefully thank Claudia Heyer, David Hallmann, and Ines Krause for their excellent technical support in acquiring data and data analysis.

REFERENCES

1. Kanda T, Ishii K, Kawaguchi H, et al. High signal intensity in the dentate nucleus and globus pallidus on unenhanced T1-weighted MR images: relationship with increasing cumulative dose of a gadolinium-based contrast material. *Radiology*. 2014;270:834–841. doi:10.1148/radiol.13131669.
2. Cao Y, Huang DQ, Shih G, et al. Signal change in the dentate nucleus on T1-weighted MR images after multiple administrations of gadopentetate dimeglumine versus gadobutrol. *AJR Am J Roentgenol*. 2016;206:414–419. doi:10.2214/AJR.15.15327.
3. Errante Y, Cirimele V, Mallio CA, et al. Progressive increase of T1 signal intensity of the dentate nucleus on unenhanced magnetic resonance images is associated with cumulative doses of intravenously administered gadodiamide in patients with normal renal function, suggesting dechelation. *Invest Radiol*. 2014;49:685–690. doi:10.1097/RLI.0000000000000072.
4. McDonald RJ, McDonald JS, Kallmes DF, et al. Intracranial gadolinium deposition after contrast-enhanced MR imaging. *Radiology*. 2015;275:772–782. doi:10.1148/radiol.15150025.
5. Radbruch A, Weberling LD, Kieslich PJ, et al. Intraindividual analysis of signal intensity changes in the dentate nucleus after consecutive serial applications of linear and macrocyclic gadolinium-based contrast agents. *Invest Radiol*. 2016;51:683–690. doi:10.1097/RLI.0000000000000308.
6. Ramalho J, Castillo M, AlObaidy M, et al. High signal intensity in globus pallidus and dentate nucleus on unenhanced T1-weighted MR images: evaluation of two linear gadolinium-based contrast agents. *Radiology*. 2015;276:836–844. doi:10.1148/radiol.2015150872.
7. Robert P, Lehericy S, Grand S, et al. T1-weighted hypersignal in the deep cerebellar nuclei after repeated administrations of gadolinium-based contrast agents in healthy rats: difference between linear and macrocyclic agents. *Invest Radiol*. 2015;50:473–480. doi:10.1097/RLI.0000000000000181.
8. Roberts DR, Chatterjee AR, Yazdani M, et al. Pediatric patients demonstrate progressive T1-weighted hyperintensity in the dentate nucleus following multiple doses of gadolinium-based contrast agent. *AJNR Am J Neuroradiol*. 2016;37:2340–2347. doi:10.3174/ajnr.A4891.

© 2022 The Author(s). Published by Wolters Kluwer Health, Inc.

9. Stojanov DA, Aracki-Trenkic A, Vojinovic S, et al. Increasing signal intensity within the dentate nucleus and globus pallidus on unenhanced T1W magnetic resonance images in patients with relapsing-remitting multiple sclerosis: correlation with cumulative dose of a macrocyclic gadolinium-based contrast agent, gadobutrol. *Eur Radiol*. 2016;26:807–815. doi:10.1007/s00330-015-3879-9.
10. Weberling LD, Kieslich PJ, Kickingereder P, et al. Increased signal intensity in the dentate nucleus on unenhanced T1-weighted images after gadobenate dimeglumine administration. *Invest Radiol*. 2015;50:743–748. doi:10.1097/RLI.0000000000000206.
11. Jost G, Frenzel T, Boyken J, et al. Gadolinium presence in the brain after administration of the liver-specific gadolinium-based contrast agent gadoxetate: a systematic comparison to multipurpose agents in rats. *Invest Radiol*. 2019;54:468–474. doi:10.1097/RLI.0000000000000559.
12. Kanda T, Nakai Y, Oba H, et al. Gadolinium deposition in the brain. *Magn Reson Imaging*. 2016;34:1346–1350. doi:10.1016/j.mri.2016.08.024.
13. Kanda T, Oba H, Toyoda K, et al. Brain gadolinium deposition after administration of gadolinium-based contrast agents. *Jpn J Radiol*. 2016;34:3–9. doi:10.1007/s11604-015-0503-5.
14. Robert P, Fingerhut S, Factor C, et al. One-year retention of gadolinium in the brain: comparison of gadodiamide and gadoterate meglumine in a rodent model. *Radiology*. 2018;288:424–433. doi:10.1148/radiol.2018172746.
15. Mallio CA, Lo Vullo G, Messina L, et al. Increased T1 signal intensity of the anterior pituitary gland on unenhanced magnetic resonance images after chronic exposure to gadodiamide. *Invest Radiol*. 2020;55:25–29. doi:10.1097/RLI.0000000000000604.
16. Jost G, Lenhard DC, Sieber MA, et al. Signal increase on unenhanced T1-weighted images in the rat brain after repeated, extended doses of gadolinium-based contrast agents: comparison of linear and macrocyclic agents. *Invest Radiol*. 2016;51:83–89. doi:10.1097/RLI.0000000000000242.
17. Bjornerud A, Vatnehol SAS, Larsson C, et al. Signal enhancement of the dentate nucleus at unenhanced MR imaging after very high cumulative doses of the macrocyclic gadolinium-based contrast agent gadobutrol: an observational study. *Radiology*. 2017;285:434–444. doi:10.1148/radiol.2017170391.
18. Boyken J, Frenzel T, Lohrke J, et al. Gadolinium accumulation in the deep cerebellar nuclei and globus pallidus after exposure to linear but not macrocyclic gadolinium-based contrast agents in a retrospective pig study with high similarity to clinical conditions. *Invest Radiol*. 2018;53:278–285. doi:10.1097/RLI.0000000000000440.
19. Jost G, Frenzel T, Boyken J, et al. Long-term excretion of gadolinium-based contrast agents: linear versus macrocyclic agents in an experimental rat model. *Radiology*. 2019;290:340–348. doi:10.1148/radiol.2018180135.
20. Kanda T, Osawa M, Oba H, et al. High signal intensity in dentate nucleus on unenhanced T1-weighted MR images: association with linear versus macrocyclic gadolinium chelate administration. *Radiology*. 2015;275:803–809. doi:10.1148/radiol.14140364.
21. Radbruch A, Weberling LD, Kieslich PJ, et al. Gadolinium retention in the dentate nucleus and globus pallidus is dependent on the class of contrast agent. *Radiology*. 2015;275:783–791. doi:10.1148/radiol.2015150337.
22. Robert P, Violas X, Grand S, et al. Linear gadolinium-based contrast agents are associated with brain gadolinium retention in healthy rats. *Invest Radiol*. 2016;51:73–82. doi:10.1097/RLI.0000000000000241.
23. Zhang Y, Cao Y, Shih GL, et al. Extent of signal hyperintensity on unenhanced T1-weighted brain MR images after more than 35 administrations of linear gadolinium-based contrast agents. *Radiology*. 2017;282:516–525. doi:10.1148/radiol.2016152864.
24. European Medicines Agency. EMA's final opinion confirms restrictions on use of linear gadolinium agents in body scans. 2017. Available at: https://www.ema.europa.eu/documents/referral/gadolinium-article-31-referral-emas-final-opinion-confirmsrestrictions-use-linear-gadolinium-agents_en.pdf. Accessed January 20, 2021.
25. Frenzel T, Apte C, Jost G, et al. Quantification and assessment of the chemical form of residual gadolinium in the brain after repeated administration of gadolinium-based contrast agents: comparative study in rats. *Invest Radiol*. 2017;52:396–404. doi:10.1097/RLI.0000000000000352.
26. Runge VM. Dechelation (transmetalation): consequences and safety concerns with the linear gadolinium-based contrast agents, in view of recent health care rulings by the EMA (Europe), FDA (United States), and PMDA (Japan). *Invest Radiol*. 2018;53:571–578. doi:10.1097/RLI.0000000000000507.
27. Bussi S, Coppo A, Botteron C, et al. Differences in gadolinium retention after repeated injections of macrocyclic MR contrast agents to rats. *J Magn Reson Imaging*. 2018;47:746–752. doi:10.1002/jmri.25822.
28. Radbruch A. Gadolinium deposition in the brain: we need to differentiate between chelated and dechelated gadolinium. *Radiology*. 2018;288:434–435. doi:10.1148/radiol.2018180294.
29. Runge VM. Macrocyclic versus linear gadolinium chelates. *Invest Radiol*. 2015;50:811. doi:10.1097/RLI.0000000000000229.
30. Deike-Hofmann K, Reuter J, Haase R, et al. No changes in T1 relaxometry after a mean of 11 administrations of gadobutrol. *Invest Radiol*. 2020;55:381–386. doi:10.1097/RLI.0000000000000650.
31. Kang KM, Choi SH, Hwang M, et al. T1 shortening in the globus pallidus after multiple administrations of gadobutrol: assessment with a multidynamic multiecho sequence. *Radiology*. 2018;287:258–266. doi:10.1148/radiol.2017162852.
32. Saake M, Schmidle A, Kopp M, et al. MRI brain signal intensity and relaxation times in individuals with prior exposure to gadobutrol. *Radiology*. 2019;290:659–668. doi:10.1148/radiol.2018181927.
33. Muller A, Jurcoane A, Madler B, et al. Brain relaxometry after macrocyclic Gd-based contrast agent. *Clin Neuroradiol*. 2017;27:459–468. doi:10.1007/s00062-017-0608-6.
34. Tedeschi E, Palma G, Canna A, et al. In vivo dentate nucleus MRI relaxometry correlates with previous administration of gadolinium-based contrast agents. *Eur Radiol*. 2016;26:4577–4584. doi:10.1007/s00330-016-4245-2.
35. Splendiani A, Corridore A, Torlone S, et al. Visible T1-hyperintensity of the dentate nucleus after multiple administrations of macrocyclic gadolinium-based contrast agents: yes or no? *Insights Imaging*. 2019;10:82. doi:10.1186/s13244-019-0767-x.
36. Radbruch A, Haase R, Kieslich PJ, et al. No signal intensity increase in the dentate nucleus on unenhanced T1-weighted MR images after more than 20 serial injections of macrocyclic gadolinium-based contrast agents. *Radiology*. 2017;282:699–707. doi:10.1148/radiol.2016162241.
37. Radbruch A, Weberling LD, Kieslich PJ, et al. High-signal intensity in the dentate nucleus and globus pallidus on unenhanced T1-weighted images: evaluation of the macrocyclic gadolinium-based contrast agent gadobutrol. *Invest Radiol*. 2015;50:805–810. doi:10.1097/RLI.0000000000000227.
38. Jost G, Frenzel T, Boyken J, et al. Impact of brain tumors and radiotherapy on the presence of gadolinium in the brain after repeated administration of gadolinium-based contrast agents: an experimental study in rats. *Neuroradiology*. 2019;61:1273–1280. doi:10.1007/s00234-019-02256-3.
39. Saake M, Hepp T, Schmidle A, et al. Influence of artifact corrections on MRI signal intensity ratios for assessment of gadolinium brain retention. *Acad Radiol*. 2020;27:744–749. doi:10.1016/j.acra.2019.07.013.
40. Young LK, Gandy SJ, Priba L, et al. The impact of different magnetic resonance imaging equipment and scanning parameters on signal intensity ratio measurements in phantoms and healthy volunteers: implications for interpreting gadolinium signal changes within the brain. *Invest Radiol*. 2019;54:169–176. doi:10.1097/RLI.0000000000000526.
41. Boyken J, Niendorf T, Flemming B, et al. Gadolinium deposition in the brain after contrast-enhanced MRI: are the data valid? *Radiology*. 2018;288:630–632. doi:10.1148/radiol.2018171762.
42. Quattrocchi CC, Errante Y, Mallio CA, et al. Effect of age on high T1 signal intensity of the dentate nucleus and globus pallidus in a large population exposed to gadodiamide. *Invest Radiol*. 2018;53:214–222. doi:10.1097/RLI.0000000000000431.
43. Krug KB, Burke CJ, Weiss K, et al. Influence of aging and gadolinium exposure on T1, T2, and T2*-relaxation in healthy women with an increased risk of breast cancer with and without prior exposure to gadoterate meglumine at 3.0-T brain MR imaging. *Eur Radiol*. 2022;32:331–345. doi:10.1007/s00330-021-08069-4.
44. Badve C, Yu A, Rogers M, et al. Simultaneous T1 and T2 brain relaxometry in asymptomatic volunteers using magnetic resonance fingerprinting. *Tomography*. 2015;1:136–144. doi:10.18383/j.tom.2015.00166.
45. Valdés Hernandez Mdel C, Maconick LC, Tan EM, et al. Identification of mineral deposits in the brain on radiological images: a systematic review. *Eur Radiol*. 2012;22:2371–2381. doi:10.1007/s00330-012-2494-2.
46. Kupeli A, Kocak M, Goktepeli M, et al. Role of T1 mapping to evaluate brain aging in a healthy population. *Clin Imaging*. 2020;59:56–60. doi:10.1016/j.clinimag.2019.09.005.
47. Flood TF, Bhatt PR, Jensen A, et al. Age-dependent signal intensity changes in the structurally normal pediatric brain on unenhanced T1-weighted MR imaging. *AJNR Am J Neuroradiol*. 2019;40:1824–1828. doi:10.3174/ajnr.A6254.
48. Harder SL, Hopp KM, Ward H, et al. Mineralization of the deep gray matter with age: a retrospective review with susceptibility-weighted MR imaging. *AJNR Am J Neuroradiol*. 2008;29:176–183. doi:10.3174/ajnr.A0770.
49. Kanda T, Nakai Y, Aoki S, et al. Contribution of metals to brain MR signal intensity: review articles. *Jpn J Radiol*. 2016;34:258–266. doi:10.1007/s11604-016-0532-8.
50. Knight MJ, McCann B, Tsivos D, et al. Quantitative T1 and T2 MRI signal characteristics in the human brain: different patterns of MR contrasts in normal ageing. *MAGMA*. 2016;29:833–842. doi:10.1007/s10334-016-0573-0.
51. Maschke M, Weber J, Dimitrova A, et al. Age-related changes of the dentate nuclei in normal adults as revealed by 3D fast low angle shot (FLASH) echo sequence magnetic resonance imaging. *J Neurol*. 2004;251:740–746. doi:10.1007/s00415-004-0420-5.
52. Ogg RJ, Steen RG. Age-related changes in brain T1 are correlated with iron concentration. *Magn Reson Med*. 1998;40:749–753. doi:10.1002/mrm.1910400516.

© 2022 The Author(s). Published by Wolters Kluwer Health, Inc.

53. Zhuang FJ, Chen Y, He WB, et al. Prevalence of white matter hyperintensities increases with age. *Neural Regen Res*. 2018;13:2141–2146. doi:10.4103/1673-5374.241465.
54. Lohrke J, Frisk AL, Frenzel T, et al. Histology and gadolinium distribution in the rodent brain after the administration of cumulative high doses of linear and macrocyclic gadolinium-based contrast agents. *Invest Radiol*. 2017;52:324–333. doi:10.1097/RLI.0000000000000344.
55. Forslin Y, Martola J, Bergendal A, et al. Gadolinium retention in the brain: an MRI relaxometry study of linear and macrocyclic gadolinium-based contrast agents in multiple sclerosis. *AJNR Am J Neuroradiol*. 2019;40:1265–1273. doi:10.3174/ajnr.A6112.
56. Kuno H, Jara H, Buch K, et al. Global and regional brain assessment with quantitative MR imaging in patients with prior exposure to linear gadolinium-based contrast agents. *Radiology*. 2017;283:195–204. doi:10.1148/radiol.2016160674.
57. Agris J, Pietsch H, Balzer T. What evidence is there that gadobutrol causes increasing signal intensity within the dentate nucleus and globus pallidus on unenhanced T1W MRI in patients with RRMS? *Eur Radiol*. 2016;26:816–817. doi:10.1007/s00330-015-4019-2.
58. Stojanov DA. Reply to letter to the editor re: increasing signal intensity within the dentate nucleus and globus pallidus on unenhanced T1W magnetic resonance images in patients with relapsing-remitting multiple sclerosis: correlation with cumulative dose of a macrocyclic gadolinium-based contrast agent, gadobutrol. *Eur Radiol*. 2016;26:818–819. doi:10.1007/s00330-015-4020-9.
59. Gunning-Dixon FM, Raz N. The cognitive correlates of white matter abnormalities in normal aging: a quantitative review. *Neuropsychology*. 2000;14:224–232. doi:10.1037//0894-4105.14.2.224.
60. Hsu JL, Leemans A, Bai CH, et al. Gender differences and age-related white matter changes of the human brain: a diffusion tensor imaging study. *Neuroimage*. 2008;39:566–577. doi:10.1016/j.neuroimage.2007.09.017.
61. Salat DH, Tuch DS, Greve DN, et al. Age-related alterations in white matter microstructure measured by diffusion tensor imaging. *Neurobiol Aging*. 2005;26:1215–1227. doi:10.1016/j.neurobiolaging.2004.09.017.
62. Westlye LT, Walhovd KB, Dale AM, et al. Life-span changes of the human brain white matter: diffusion tensor imaging (DTI) and volumetry. *Cereb Cortex*. 2010;20:2055–2068. doi:10.1093/cercor/bhp280.
63. Callaghan MF, Freund P, Draganski B, et al. Widespread age-related differences in the human brain microstructure revealed by quantitative magnetic resonance imaging. *Neurobiol Aging*. 2014;35:1862–1872. doi:10.1016/j.neurobiolaging.2014.02.008.
64. Aquino D, Bizzi A, Grisoli M, et al. Age-related iron deposition in the basal ganglia: quantitative analysis in healthy subjects. *Radiology*. 2009;252:165–172. doi:10.1148/radiol.2522081399.
65. US Food and Drug Administration. Guidance for Industry. Estimating the maximum safe starting dose in initial clinical trials for therapeutics in adult healthy volunteers. 2005. Available at: https://www.fda.gov/media/72309/download. Accessed March 2021.

© 2022 The Author(s). Published by Wolters Kluwer Health, Inc.